Renewable Energy 253 (2025) 123485



Contents lists available at ScienceDirect

Renewable Energy

journal homepage: www.elsevier.com/locate/renene

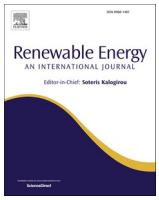



Effect of preparation method on the activity of red mud based catalysts in hydrogen production from biomass

Hakan Cay [a], Nazire Merve Akbas [b], Gozde Duman [a], Osman Simsek [a], Güray Yildiz [c], Weitao Wang [d], Xin Tu [d], Jale Yanik [a,*]

[a] Ege University, Faculty of Science, Department of Chemistry, Izmir, 35100, Türkiye
[b] Ege University, Faculty of Engineering, Department of Chemical Engineering, Izmir, 35100, Türkiye
[c] Izmir Institute of Technology, Faculty of Engineering, Department of Energy Systems Engineering, Urla, 35430, Izmir, Türkiye
[d] Department of Electrical Engineering and Electronics, University of Liverpool, Liverpool, L69 3GJ, UK

ARTICLE INFO

Keywords:
Catalytic steam gasification
Olive tree pruning
Red mud
Plasma activation

ABSTRACT

Biomass gasification is a promising technology for hydrogen production. This study presents H_2 production from olive tree pruning (OTP), employing a fixed dual-bed reactor that combines OPT gasification and volatile reforming. The thermal steam gasification of OTP was performed at 850 °C, followed by the catalytic gasification of volatiles at different temperatures. Red mud (RM) and nickel loaded red mud (Ni-RM) catalysts were used as catalytic bed material.

The effects of different operating parameters, i.e. catalytic bed temperature, catalyst preparation method (thermal reduction & plasma reduction), and nickel ratios in catalyst on the yield and composition of produced gases were investigated. The catalyst prepared by reduction under non-thermal plasma showed no effect on the gasification due to the insufficient temperature for the reduction of Fe_2O_3 and NiO. The results indicated that the bottom bed temperature had a significant effect on the H_2 yield, especially in the catalytic experiments. The RM alone shows almost the same activity with Ni-RM on the H_2 yield; 1076 mL gas/g OTP and 1128 mL gas/g OTP, respectively. The results of present study showed that reduced RM had as much catalytic activity as Ni loaded reduced RM in hydrogen production.

1. Introduction

Population growth, modernization, and industrialization have all led to a significant increase in energy consumption and related demand. Fossil fuels have been the main resource for this demand causing climate change and greenhouse gas emissions, which has led researchers to look for eco-friendly, renewable, and sustainable energy sources. Hydrogen (H_2) is coming up as one of the cleanest and most carbon-neutral future energy carriers and has a high calorific value of 122 kJ/g, having a 2.75-fold higher heating efficiency than that of the hydrocarbons [1].

H_2 production from biomass, the most abundant energy source, is receiving increasing attention due to its carbon neutrality, sustainability and environmental friendliness through both biochemical and thermochemical processes. The thermochemical route for producing hydrogen from biomass has shown great potential for industrial implementation. This route uses heat to break down the biomass into hydrogen and other gases. It is a more efficient and sustainable way to produce H_2 than other methods [2].

Among the thermochemical routes, steam gasification is one of the efficient ways to produce the highest yields of hydrogen due to the water–gas-shift, steam reforming and water–gas reactions. The main problem of gasification in general is the tar formed during the pyrolysis step, representing the main barrier for the commercial breakthrough of gasification technologies. Tar reduction/removal technologies can be classified into two categories: The physical methods including scrubber, filter, cyclone and electrostatic precipitator are applied in the downstream of gasification. The secondary methods include optimisation of the gasifier design, the gasification operation conditions and addition of catalytic bed materials. Currently, the catalytic cracking of tar has become the main focus for tar removal due to the increase in quality of gas and therefore increasing gasification efficiency [3]. In literature, numbers of catalysts have been tested to crack the tar either in-situ or ex-situ [4].

The catalyst must be inexpensive, capable of functioning in all

* Corresponding author.
E-mail address: jale.yanik@ege.edu.tr (J. Yanik).

https://doi.org/10.1016/j.renene.2025.123485
Received 19 January 2025; Received in revised form 12 May 2025; Accepted 16 May 2025
Available online 19 May 2025
0960-1481/© 2025 Published by Elsevier Ltd.

reaction environments (i.e. high temperature and pressure) and increasing the yield of the desired product, resistant to sintering, and able to be regenerated after use. Nickel is a highly active catalyst that is widely used in steam-reforming reactions. Nickel is also relatively inexpensive, making it a cost-effective choice for related industrial applications [5]. Ni-based catalysts can break down the C–H, C–C, and O–H bonds in oxygenated compounds derived from pyrolysis/gasification of biomass and favour the production of H_2, CO, and CO_2 at high temperatures [6]. Fe-based catalysts, on the other hand, are widely used in the gasification of biomass because they have a variable valence, are highly active, easy to obtain, and environmentally friendly [7,8]. It was found that the metallic iron is more active in cracking of tar produced from gasification, compared to corresponding oxides [9]. This is because the reduced state of iron has more electrons available to participate in the reaction. Therefore, a prior reduction step is usually needed to improve the catalytic activity of Fe-based catalysts [10]. In addition to the active metal, the selection of an appropriate catalyst support is another critical technical consideration in the construction of high-performance catalysts used in the steam gasification of biomass [11].

Red mud (RM) is a solid waste generated during alumina production from bauxite by Bayer process. The global production of RM is thought to be between 120 and 150 million tons per year [12]. It contains mainly the oxides of iron, aluminium, silicon and alkaline metals. Due to the complex composition of RM, several key factors need to be taken into account to explain its catalytic effect. A wide variety of metal oxides in RM are expected to provide RM with high catalytic ability in various chemical reactions. Previous studies showed that its catalytic activity is mostly attributed to its high iron content which has a certain oxygen-carrying capacity. RM as base catalysts in different thermal biomass conversion processes such as pyrolysis [13,14], catalytic cracking of tar model compounds [8,15], hydrodeoxygenation [16,17], air [18] and steam [19,20] gasification have been paid wide attention. Zhou et al. [13] investigated the catalytic mechanism of RM pyrolysis of corn stover. They reported that Fe_2O_3 in the RM is the main catalytically active contributor to the improvement of carbon conversion and hydrogen yield. The same research group [19] also performed in-situ catalytic fast steam gasification of corn stover with Fe_2O_3 and RM. Their investigation showed that RM can significantly promote the pyrolysis of biomass to produce CO and CO_2 and in the gasification stage, fixed carbon is catalyzed by Fe oxides leading to increase in H_2 and CO_2 through the water–gas shift reaction. In another study, Zhao et al. studied the co-gasification of coal and biomass to produce hydrogen-rich synthesis gas with red mud. They reported that the cyclic transformation of iron, potassium and calcium between the oxidation and reduction states promotes the water-gas shift reaction [20].

In our previous study [21], the red mud was used in steam gasification of shells (almond and walnut). Red mud was found to be less active in tar decomposition compared to the synthesized iron-ceria catalyst due to the inhibition of iron oxide activity by sodium aluminium silicate hydrate. We also tested red mud in the steam gasification of biochar and hydrochar derived from spent coffee waste [22]. Although gas yields did not change significantly in the presence of RM in case of hydrochar, RM showed catalytic effect in case of biochar. It is worth noting that, in our previous studies [21,22], RM exhibited limited activity at catalyst bed temperatures lower than 800 °C. These findings highlight a research need in the modification of red mud catalysts for improved activity at relatively lower temperatures.

The presence of bimetallic active centers in catalyst improves the catalytic activity of catalysts for reforming of tar [24]. Nickel catalysts have been confirmed highly active for tar decomposition and cracking [25]. Although nickel-based catalysts have high tar removal activity and enhanced gas product quality, carbon deposition and sintering are their main drawbacks. Due to its stable and anti-poisoning characteristics, RM can improve the sensitivity of nickel-based catalysts to sintering and poisoning. The main chemical components of RM can be divided into two categories according to their role in the catalytic process: active component (Fe_2O_3) and inert carriers (Al_2O_3, SiO_2). The red mud supported metal catalyst can be more effective than red mud alone. More recently, Dong et al. [23] used nickel loaded RM to produce hydrogen-rich gas from bamboo sawdust. And they found that a 10 % addition of nickel gave the best performance with the enhancing 32.7 % syngas and 43.8 % hydrogen yield.

The catalytic performance of nickel-based catalysts is highly dependent on their oxidation states. Metallic nickel is mostly recognized as active form in tar decomposition [26]. Reduction of these catalysts can be achieved through various methods, including carbothermal reduction [26], thermal [17] and plasma-assisted reduction [27,28] under a reductive atmosphere such as hydrogen. Since the 1990s, using plasma for catalysis has attracted a lot of attention. The use of various plasma in catalyst preparation provides better control size and structure, improving catalytic properties [29,30]. The non-thermal plasma process is a developing technology that uses electricity to generate plasma by applying a large potential difference across two electrodes. In non-thermal plasma, H_2 is transformed into reactive species such as electrons, photons, excited hydrogen molecules (H_2*), atomic hydrogen (H), and hydrogen ions (H^+). Although their formation requires high energy ($\Delta G \gg 0$), these species significantly enhance the reduction of metal oxides by lowering the Gibbs free energy ($\Delta G \ll 0$), making the process more thermodynamically favorable, even at low temperatures [31]. One example of this process is the dielectric barrier discharge (DBD). Previous research by Tu et al., who studied plasma-assisted reduction of a NiO/Al_2O_3 in a H_2/Ar DBD at low temperature (<300 °C), has shown that combining plasma with a catalyst can create a synergistic effect [27]. They concluded that this synergistic effect can significantly reduce the activation temperature of the catalyst, improve its activity and stability, and ultimately increase the conversion of energy efficiency to produce target gas products. In another study, Lian et al. prepared the Ni- $LaFeO_3$ catalyst using DBD in H_2/Ar atmosphere for use in hydrogen production by steam reforming of methane [28]. They concluded that plasma treatment can improve the interaction between the active nickel sites and the support material. This leads to a higher dispersion of nickel on the support, which in turn improves the activity and coke resistance of the catalyst for hydrogen-rich gas production. Although, there are few studies present in the literature relating to Ni-based catalyst prepared by DBD, as far as the authors know, there is no research on plasma-assisted reduction of Ni-loaded iron-based catalyst.

One of the key considerations in selecting biomass as a feedstock for gasification is its regional availability and abundance, as locally sourced biomass can reduce the transportation costs and minimize the risk of supply chain disruptions. Olive tree groves are a common sight in the Mediterranean basin, and they produce a significant amount of biomass waste. The pruning produced from Southern European countries amount to around 5.5 million tonnes (dry basis) [32]. This is because the demand for olive oil is increasing due to the health benefits associated with its consumption. On the other hand, this huge amount of waste brings several problems, e.g. disposal and uncontrolled burning in open fields [33]. Hence, the use of olive tree pruning (OTP) as biomass feedstock makes a significant contribution to sustainable development [34].

After a careful review of previous studies, red mud appears to be a promising catalyst for steam gasification. Nevertheless, there remains a research gap in improvement of its performance through the addition of active metals, such as Ni, and the reduction of these active metal species. This study presents a novel preparation of RM-based catalysts for hydrogen-rich gas production in OTP steam gasification. Unlike our previous studies [21,22] and other gasification studies in the literature, we investigated the reduction of red mud with thermal and plasma methods as pretreatment to increase its catalytic activity at low temperatures. The objectives of present study are: 1) To compare the catalytic activities of RM-based catalysts prepared by plasma and conventional thermal processes on steam reforming of volatiles in

biomass gasification. 2) to investigate the effect of Ni loading on the catalytic activity of RM in steam reforming of volatiles. To the best of authors' knowledge, the use of non-thermal plasma-assisted reduction of RM as catalyst in steam gasification of biomass has not been investigated so far. This study provides a new way to use RM as a catalyst in biomass gasification.

2. Materials and methods

2.1. Biomass and characterization

Olive tree pruning (OTP) was selected as the reference biomass feedstock; which consists of the branches, shoots (with a diameter of less than 5 cm) and leaves of olive tree. OTP was collected from a field located on the Ege University campus in Izmir, Türkiye, during the pruning season (december). Approximately 25–30 kg of OTP was collected and then shredded using a miller to achieve a particle size smaller than 2 cm, followed by oven-drying at 110 °C to prevent decay and biological degradation. Finally, the dried samples were ground to a particle size of less than 0.5 mm in a laboratory scale blade miller (Polymix PX-MFC 90 D Kinematica AD) and stored in a sealed plastic container. The elemental analysis of biomass was carried out using a CHNS-932 analyzer (LECO) according to ASTM D5373–16 [35]. The ash and volatile matter contents were determined according to NREL/TP-510- 42622 [36] and ASTM D3175-89a [37], respectively. The higher heating value (HHV) of raw material was measured by the following equation [38];

$$HHV\,[MJ/kg] = 0.3491xC + 1.1783xH + 0.1005xS - 0.1034xO - 0.0151xN - 0.0211xAsh \quad (1)$$

Some properties of OTP are given in Table 1.

2.2. Preparation of catalysts and characterization

Red mud (a by-product of the production of aluminium from bauxite) was utilized as the base catalyst. Red mud (RM) was supplied in powder form from an alumina refinery in Seydişehir, Turkey. To increase the surface area and to remove the soluble alkali metal ions, RM was boiled in 3 M HCl for 2 h. NH_4OH was added dropwise to the slurry with slow stirring until the pH reached 8. The slurry was then centrifuged and filtrated, the precipitate was washed 3 times with distilled water and the centrifugation process was repeated. The precipitate was calcined at 550 °C for 2 h after being dried at 105 °C. The obtained solid was named the "activated red mud" (ARM).

Table 1
Properties of olive tree pruning.

Proximate analysis (*wt.*%, d.b.)	
Fixed carbon	21.8(±0.1)
Volatile matter	72.3 (±0.2)
Ash	5.9(±0.1)
Ultimate analysis (*wt.*%, d.b.)	
C	49.98(±1.70)
H	6.45(±0.41)
O*	35.65 (±2.21)
N	1.88 (±0.18)
S	0.18 (±0.02)
HHV [MJ/kg]	21.17(±1.32)

d.b.: dry basis.
O*, % = 100 - [C + H + N + S + Ash]% [39].

Ni-loaded ARM catalysts were prepared by the wetness impregnation method. ARM catalysts (particle size <90 μm) were mixed with Ni $(NO_3).6H_2O$ solution at 2.5 %, 5.0 %, 7.5 % and 10.0 % by weight of Ni. The mixture was stirred continuously for 3.5 h at 70 °C. It was then dried at 105 °C for 12 h and calcined accordingly at 550 °C for 2 h.

Both ARM and the Ni loaded ARM catalysts were reduced with H_2 by two methods, namely, thermal treatment and non-thermal plasma treatment.

2.2.1. Thermal treatment method

Before the experiments, the Ni-loaded catalyst was reduced with H_2 at a flow rate of 50 ml/min at 700 °C for 1 h. Catalysts were named an R-xNi-ARM (where "R" and "x" stand for "reduced" and the weight percent of Ni, respectively). For comparison purposes, ARM alone was also reduced in the same way.

2.2.2. Non-thermal plasma treatment method

Ni-loaded ARM catalysts prepared by the wetness impregnation method and dried at 105 °C were treated by plasma for 1h in the presence of a 10 % H_2-Ar gas mixture with a 100 mL flow rate. For comparison purposes, ARM alone was also treated in the same way. Fig. S1 shows the DBD reactor system used for the plasma treatment. More details regarding the configuration of the DBD reactor system are available in a previous study [40].

In a typical plasma treatment run, catalyst pellets weighing 3 g were packed into the plasma region along the bottom of the quartz tube, partially filling the discharge gap and held by quartz wood. The quartz wood was placed outside the plasma region to avoid its effect on the plasma chemical reactions. In this work, the frequency was fixed at 12 kHz and the temperature was 140 °C. After the plasma process, the catalyst was named a P-R-xNi-ARM (where P stands for "Plasma").

2.2.3. Characterization of catalysts

X-Ray Fluorescence Spectrometry (XRF) measurements were performed with a Spectro-IQ II (Kleve, Germany). X-ray powder diffraction (XRD) analysis were carried out by a Philips X'Pert Pro (Almelo, The Netherlands) powder diffractometer equipped with a Cu anode X-ray source (CuK_α = 1.5406 Å at 45 kV, 40 mA). All XRD patterns were obtained at a scan range of 5–80°, scan step size of 0.02 and 5 s per step.

To determine the surface area of the catalysts, the Brunauer–Emmett–Teller (BET) measurements were performed based on the nitrogen (N_2) gas adsorption technique in a liquid nitrogen environment at 77 K. After the catalysts were degassed at 300 °C for 3 h, N_2 adsorption measurements were made in the with a Micromeritics Gemini V (Micromeritics, Norcross, GA, USA). The surface morphology of catalysts was analyzed by SEM (ETD detector with Thermo Scientific Apreo S).

2.3. Steam gasification

Steam gasification of OTP was carried out in a fixed dual-bed gasification reactor system, illustrated in Fig. 1. The reactor is made of stainless steel, with an inner diameter of 6 cm and a length of 100 cm. It consists of two separate heating zones, located 15 mm from the top and bottom ends of the reactor, each heated by individual electric furnaces that allow each bed zone to reach different temperatures with different heating rates. The temperature of the top zone is monitored using a type K thermocouple. A detailed explanation of the experimental setup was given in our previous publication [22]. Steam gasification experiments

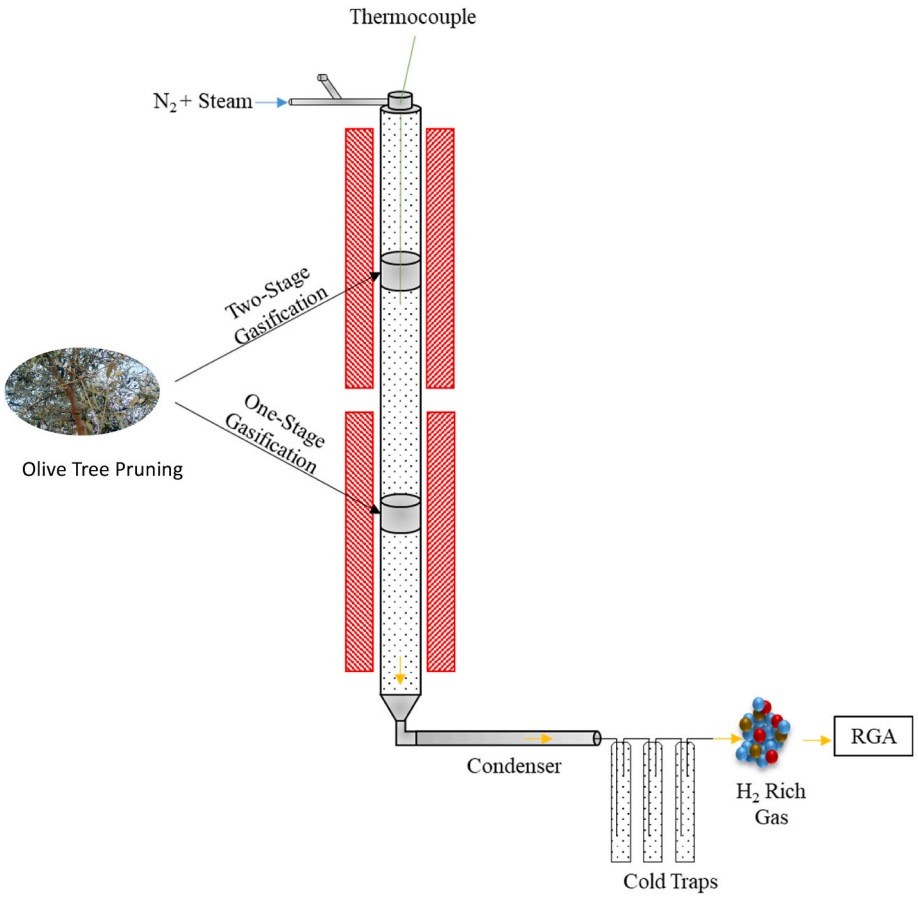

Fig. 1. Schematic of the laboratory-scale dual-bed gasification system.

Table 2
XRF analysis data of catalysts (%).

	RM	ARM	7.5 Ni-ARM
Fe_2O_3	23.98 (±0.04)	40.81 (±0.05)	38.23 (±0.05)
Al_2O_3	24.81 (±0.05)	41.69 (±0.07)	34.83(±0.07)
Na_2O	17.04 (±0.33)	4.79 (±0.40)	3.46 (±0.38)
CaO	28.41 (±0.04)	2.81 (±0.01)	2.51(±0.01)
NiO	0.05 (±0.00)	0.07 (±0.00)	12.54 (±0.03)
TiO_2	3.81 (±0.05)	6.72 (±0.02)	6.19 (±0.01)
MgO	1.29 (±0.05)	1.08 (±0.40)	1.19 (±0.06)

were performed using two configurations within the same system. In a two-stage catalytic gasification, 3 g of the biomass was placed in the upper bed basket and 3 g of catalyst was placed in the bottom bed basket while two-stage thermal steam gasification was conducted without catalyst loading in the bottom bed. In case of one-stage steam gasification, only 3 g of biomass was placed in the bottom bed without mixing a catalyst; thereby, no thermal cracking of tar occurred.

First, the bottom bed was heated to the desired temperature, then the upper bed was heated to 850 °C with a heating rate of 8 °C/min and held at that temperature for 1 h. The experiments were carried out under a nitrogen flow of 100 mL/min, which is fed from the upper part of the reactor. When the upper bed temperature reaches 200 °C, steam (0.5 mL/min) is supplied to the reactor along with nitrogen gas. The upper bed temperature, nitrogen and steam flow rates were chosen according to our previous studies [22]. The volatile products released during the gasification process were passed through the condenser and two ice traps and collected in the Tedlar bag.

2.4. Analysis of gas products

Gas products collected in the Tedlar bag were analyzed by Refinery Gas Analyser (RGA, Agilent Technologies 7890A GC System). This instrument is configured to analyze the gas products within 12.6 min. The system has five valves and three detectors. The FID channel is configured to analyze hydrocarbons from C_1 to C_5. The first TCD channel (reference gas He) is configured to detect permanent gases which include CO_2, CO, O_2, and N_2. The second TCD channel (with reference gas N_2) is dedicated to analysing the hydrogen. Gas products were identified and quantified according to the standard gas mixture (Agilent P/N 5190-0519) by using external calibration method.

Table 3
BET analysis data of catalysts.

Catalyst	S_{BET}, m^2/g	S_{Ext}, m^2/g	S_{micro}, m^2/g	V_T, cm^3/g	D_{av}, nm
RM	10.38	8.31	2.07	0.13	50.41
ARM	169.99	169.99	–	0.44	10.45
R-ARM	35.18	32.77	2.41	0.24	26.90
R-7.5Ni-ARM	81.14	80.48	0.66	0.38	18.84
S-R-7.5Ni-ARM	50.14	48.37	1.77	0.32	25.27
P-R-7.5Ni-ARM	45.61	45.48	0.13	0.17	15.13
S-P-R-7.5Ni-ARM	48.39	47.20	1.19	0.14	11.67

N_2 adsorption tests for some catalysts were replicated twice. The relative standard deviation (RSD) values for S_{BET}, S_{ext}, V_T, and D_{av} were found to be less than 2.5 %, 6.0 %, 6.5 %, and 4.5 %, respectively.

3. Results and discussions

3.1. Catalyst characteristics

The main compounds of raw- and activated- Red Mud are presented in Table 2. After acid treatment, the contents of Na and Ca decreased significantly, while contents of Fe, Al and Ti increased significantly. On the other hand, Ni and Mg contents remained the same as their levels in raw red mud. Since Na and Ca oxides cause the catalysts to sinter at high temperatures, resulting in a decrease in the acidity of the catalyst, it can be concluded that the ARM catalyst has a certain resistance to sintering and suitable acidity [**14**].

The surface area of RM, which was 10.4 m^2/g, increased to 169.99 m^2/g after activation (Table 3). The reason is that the acid-alkali treatment led to the formation of new pore by removing sodium and calcium ions. In addition, Wang et al. [14]. reported that calcination improved the surface area and pore structure due to elimination of some volatile matters. On the other hand, reduction of H_2 significantly reduced the surface area of the ARM (from 169.99 m^2/g to 35.18 m^2/g). A similar reduction in surface area was reported by Costa et al. [41]. They explained that this decrease was mainly due to fragmentation of Al-hydroxides and sodalite type minerals, along with sintering effects. But, in case of reduction of Ni-ARM catalyst, the decrease in surface area by reduction is less compared to ARM. This phenomenon may be attributed to the formation of pores during the reduction of nickel oxide to metallic nickel, as reported in a previous study [25]. They indicated that a higher nickel loading results in a slight increase in specific surface area, suggesting that increased nickel content may promote additional pore formation. In the case of H_2 reduction under plasma conditions, the surface area of the plasma-treated Ni-ARM catalyst was also found to be low.

The surface properties of spent catalysts are also given in Table 3. They were named as an S-R-**7.5**Ni-ARM and **S-P-R-7.5Ni-ARM** (where "S" stands for spent).

Mineralogical structure of the main elements in catalysts was investigated by XRD. The XRD patterns (Fig. 2(a) and b) show that the iron in the RM and ARM was in the form of hematite. However, after reduction with H_2 (under thermal conditions), the hematite was converted mostly to magnetite. In Ni-ARM catalysts, the XRD patterns show that reduction with H_2 under both thermal and plasma conditions converts hematite to magnetite and nickel compounds to metallic nickel.

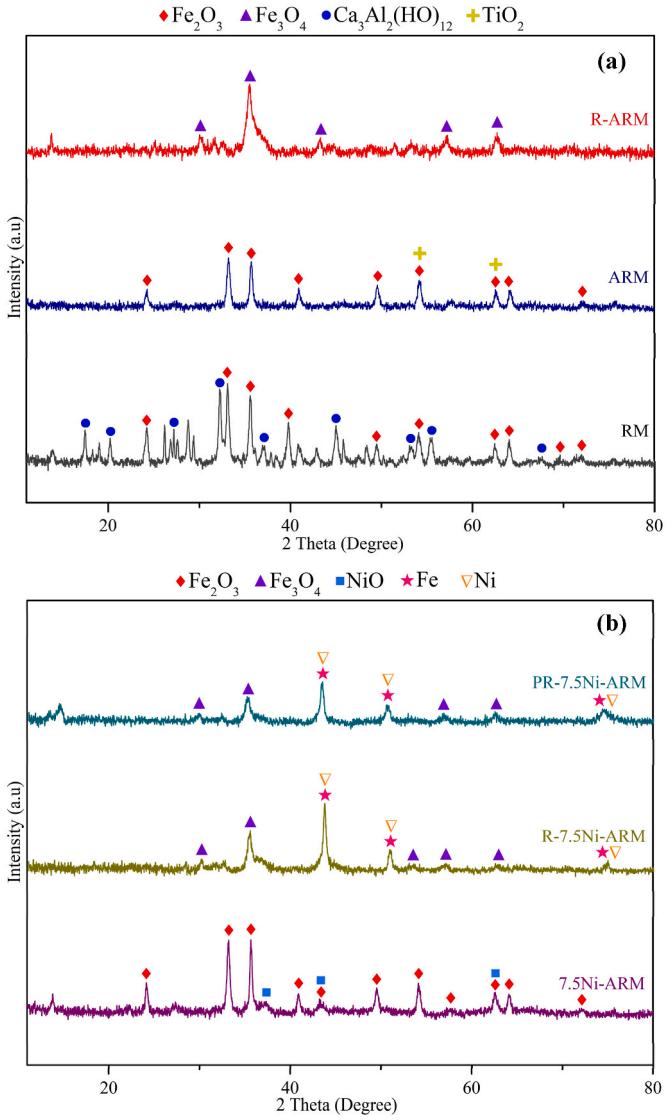

Fig. 2. XRD spectrum of red mud based catalyst (a) non-doped, (b) doped with Ni. (For interpretation of the references to colour in this figure legend, the reader is referred to the Web version of this article.)

3.2. Thermal gasification

The following reactions are expected to occur in the aforementioned in our experimental setup (dual-bed reactor) [22];

Upper bed:

200–500 °C, pyrolysis:

$$C_xH_yO_z \rightarrow \text{Char} + \text{Tar} + H_2O + \text{Gases}\ (CO_2 + CO + H_2 + CH_4 + C_{2+}) \quad (2)$$

500–850 °C

$$C + H_2O \rightarrow CO + H_2 \text{ char-steam gasification} \quad (3)$$

$$C + 2H_2O \rightarrow CH_4 \text{ methanation} \quad (4)$$

Bottom bed:

$$\text{Tar} + yH_2O \rightarrow wCO + zH_2 \text{ tar-steam reforming} \quad (5)$$

$$CO + H_2O \rightarrow CO_2 + H_2 \text{ water-gas shift} \quad (6)$$

$$CO_2 + H_2 \rightarrow CH_4 + H_2O \text{ methanation} \quad (7)$$

$$CH_4 + H_2O \rightarrow CO + 3H_2 \text{ steam-methane reforming} \quad (8)$$

Since the upper bed temperature was fixed at 850 °C, which is high enough for steam gasification of char, the bottom bed temperature is important in determining the yields and compositions of gaseous products. High temperatures promote Equations (5)–(8), which all are endothermic homogeneous gas−gas reactions, leading to tar conversion and subsequent increase in the H_2 yield. When the bottom bed temperature was increased from 700 °C to 850 °C, gas yields increased, especially H_2 yield (from 707 to 1028 mL/g OTP). To evaluate the effect of thermal reactions occurred in bottom bed on gas yield, one-stage gasification was also carried out as follows; the biomass placed in the bottom bed. First, the upper bed was heated to 200 °C, then the bottom bed started heating. The bottom bed temperature was increased up to 850 °C (at a heating rate of 8 °C/min) and held for 1 h. The effect of using a dual-bed gasifier on gas yield and composition is clearly visible in Fig. 3, H_2, CO_2 and CH_4 yields increased due to the steam reforming of the tar and other reactions (Eqs. (6)–(8)) in the bottom bed, which is consistent with the previous study [23].

It is noted that only ash remained in the upper bed at the end of gasification.

3.3. Effect of catalyst reduction process

The effect of the reduction of ARM with H_2 under thermal and

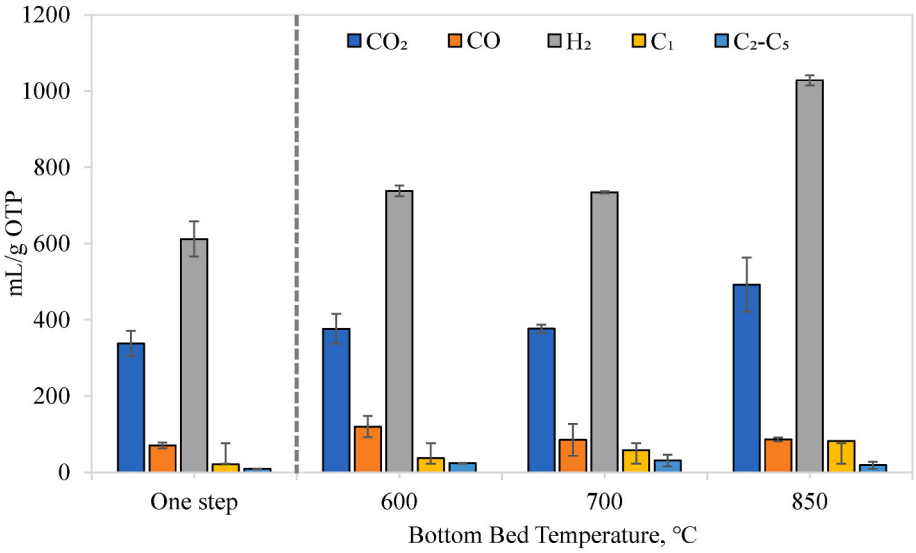

Fig. 3. Gas yields from thermal gasification of OTP by one-stage and two-stage (at varying bed temperature).

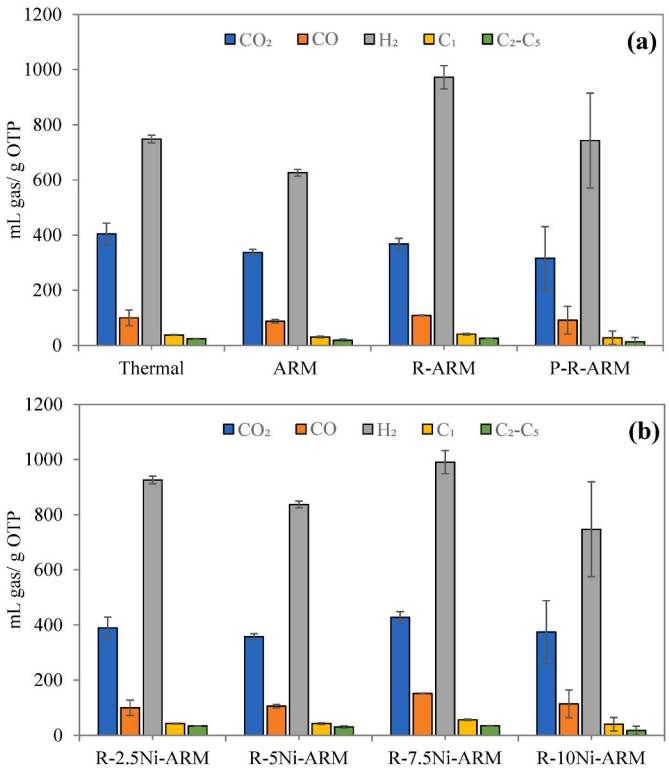

Fig. 4. Gas yields from two-step catalytic gasification of OTP at bottom bed temperature of 600 °C (a) non-doped red mud based catalyst, (b) thermal reduced Ni doped ARM catalysts, (c) plasma reduced Ni doped ARM catalysts. (For interpretation of the references to colour in this figure legend, the reader is referred to the Web version of this article.)

plasma conditions before the gasification of biomass on the gas yields of the RM-based catalysts is shown in Fig. 4(a). In these group experiments, bottom bed (catalyst bed) was kept at 600 °C to evaluate performance of the catalysts at the lowest possible temperature, thereby enhancing energy saving.

When using non-reduced catalyst, it was observed that the gas efficiency was slightly reduced compared to the thermal run. The reason for the decrease may be that the H_2 formed during gasification is consumed in the reduction of ARM. The highest H_2 yield (972 mL/g OTP) was obtained when reduced ARM (R-ARM) was used, although its surface area was much lower than ARM. Magnetite (Fe_3O_4) in the R-ARM catalyst, which can be seen in the XRD graph in Fig. 2, increased the catalytic effect compared to ARM. This result suggests that magnetite is an effective catalyst for steam reforming even at the temperature as low as 600 °C. Relevant research proved that magnetite has been more active for the water–gas shift (WGS) reaction [42].

3.4. Effect of Ni loading

As well known, Nickel-based catalysts promote tar cracking reactions at low temperatures and enhance gas product quality. Previous study has shown that that Ni loading improves the catalytic activity of red mud improving H_2 yield [23]. In Fig. 4(b), the gas yields of reduced red mud catalysts with different amounts of nickel are shown. Like in Section 3.2, bottom bed (catalyst bed) was also kept at the temperature of 600 °C in these group experiments. When Ni loading amount increased from 2.5 % to 7.5 %, the gas yields, especially H_2 yield increased compared to thermal run. However, when the Ni loading increased to 10 %, the H_2 gas yield decreased to the levels obtained in the thermal run. The reason for this may be the high rate of Ni sintering [43]. In Fig. S2, on the SEM images of R-10Ni-ARM, it was clearly seen that larger particles occur on the catalyst surface due to the sintering of small Ni metal particles. Because smaller particle size is attributable to an increase in the catalytic activity [43], the gas yields, especially the yield of H_2 decreased at Ni concentrations greater than 7.5 %. It should be noted that the hydrogen yield obtained with optimal Ni concentration (990 mL/g OTP) is almost similar to the hydrogen yield obtained using R-ARM catalyst. The reason might be that Ni loaded catalysts were not completely reduced before steam gasification experiments because R-Ni-ARM was more difficult to be reduced because of the stronger interaction of active components and the support.

3.5. Effect of plasma treatment

Non-thermal plasma reduction of catalysts has several advantages, such as improving the physical and chemical properties of the catalyst and low energy consumption due to low temperature operation.

When the gas yields obtained from ARM and Ni loaded ARM catalysts (Fig. 4(a) and (c)) prepared by using non-thermal plasma were examined, no catalytic effect of the catalysts was observed. This is because a maximum temperature of 140 °C has been reached during reduction in

non-thermal plasma treatment (Fig. S1). This temperature may not be sufficient for the reduction of Fe_2O_3, as well as the reduction of all Ni ions to elemental Ni and NO_3 ions to N_2. In addition, when the XRD graphs (Fig. 2) after thermal and plasma reduction of the 7.5 % Ni added catalyst are examined, it was seen that the magnetite and elemental Ni peak densities in PR-7.5Ni-ARM are lower than those of the R-7.5Ni-ARM. Since plasma-treated catalysts showed negligible catalytic activity, further investigations were carried out using only thermally treated catalysts.

3.6. Effect of bottom bed temperature

As discussed in Section 3.1, all reaction steps occurred at bottom are endothermic, and therefore a higher temperature promotes the cracking/reforming of hydrocarbons. As seen in Fig. 3, the highest H_2 yield (1028 mL/g OTP) was obtained at a bottom bed temperature of 850 °C in thermal run and the increase in the bottom bed temperature from 600 °C to 700 °C did not affect the H_2 yield. However, the increase in the bottom bed temperature from 600 °C to 700 °C enhanced the gas yields in catalytic runs (Fig. 5). This shows that the activity of catalysts increased with temperature.

In the presence of a R-ARM catalyst, H_2 yield increased from 972 to 1077 mL/g OTP, an incremental improvement of 11 %. In case of Ni loaded catalysts, H_2 yields increased by 21 % and 14 % for R-5Ni-ARM and R-7.5Ni-ARM, respectively, by increasing the bottom bed temperature. When the XRD graphs of R-ARM and R-7.5Ni-ARM were examined, it was observed that the intensity of the magnetite peak decreased by half when nickel was added. Based on the XRD result, it can be said that the catalytic effect is mainly due to magnetite when using R-ARM, while in the case of R-7.5Ni-ARM catalyst it is mostly caused by nickel.

Unlike the previous study [23], the hydrogen yield obtained in presence of R-7.5Ni-ARM is almost similar to the hydrogen yield obtained using R-ARM catalyst. Dong et al. [23] used nickel-loaded red mud catalyst for steam gasification of bamboo sawdust and found that the H_2 yield was significantly higher in presence of nickel-loaded red mud catalyst than that of pure RM. The difference in results is due to the catalyst preparation method. In their study, RM was used as received (without activation) and Ni impregnated RM was only calcined. But, in this study, RM was activated and then reduced with H_2 before use.

On the other hand, it can be thought that the accumulation of coke on the Ni catalyst also reduces the activity of the catalyst. It is well known that Ni-based catalysts are easily deactivated due to coke deposition [44]. To examine the coke formation on the Ni-loaded catalysts during gasification, the determination of coke amount on the catalysts after the experiments were carried out by heating them at 850 °C for 2 h in an oxygenated environment. However, as a result of combustion at 850 °C, the mass of the catalyst increased in the range of 0.26–2.1 % instead of decreasing. This might be due to the increase in mass of some samples due to oxidation of metal species. For this reason, the amount of accumulated coke could not be calculated precisely. However, when the BET results are examined (Table 3), the decrease in the surface area of the spent catalyst (S-R-7.5Ni-ARM) and the increase in the average pore diameter indicate that some coke has accumulated on the catalyst surface. Wang et al. [25] also found similar results. After the catalytic upgrading of coal pyrolysis volatiles over red mud-supported nickel catalysts, the surface area of the spent catalysts and the pore volume significantly decreased due to the carbon deposition on the surface of catalysts.

3.7. Cyclic stability and regeneration test of catalysts

One of the important aspects of the catalytic process is reusability of catalysts. In this study, the selected two catalysts (R-ARM, R-7.5Ni-ARM) were tested in catalyst reuse and regeneration experiments. A series of experiments were carried out without removing the catalyst from the bottom bed, only a new biomass sample was placed in the upper bed. As the activity of these catalysts were more pronounced at higher temperature, steam gasification was carried out at the bottom bed temperature of 700 °C. The catalyst activity decreased at the 2nd run and remained almost stable at the 3rd run. At the end of the 3rd run, it was observed that the H_2 yield decreased by approximately 30 % and 34 % (for R-ARM and R-7.5Ni-ARM, respectively) compared to that in the first run. It should be noted that the hydrogen yields obtained after five cycles are close to the yields obtained from thermal steam gasification.

To investigate regeneration performance of the spent catalysts, the spent catalyst from each run was calcined at 850 °C for 2 h and then reduced with H_2 at a flow rate of 50 ml/min at 700 °C for 1 h. The serial experiments were carried out at a bottom bed temperature of 700 °C. Experimental results are depicted in Fig. 6. In the case of gasification with R-ARM, although the H_2 yield slightly decreased in the first cycle, a hydrogen-rich gas product was obtained in subsequent trials with almost the same efficiency as the trial in which fresh catalyst was used. In the case of gasification with R-7.5Ni-ARM, the H_2 yield decreased by

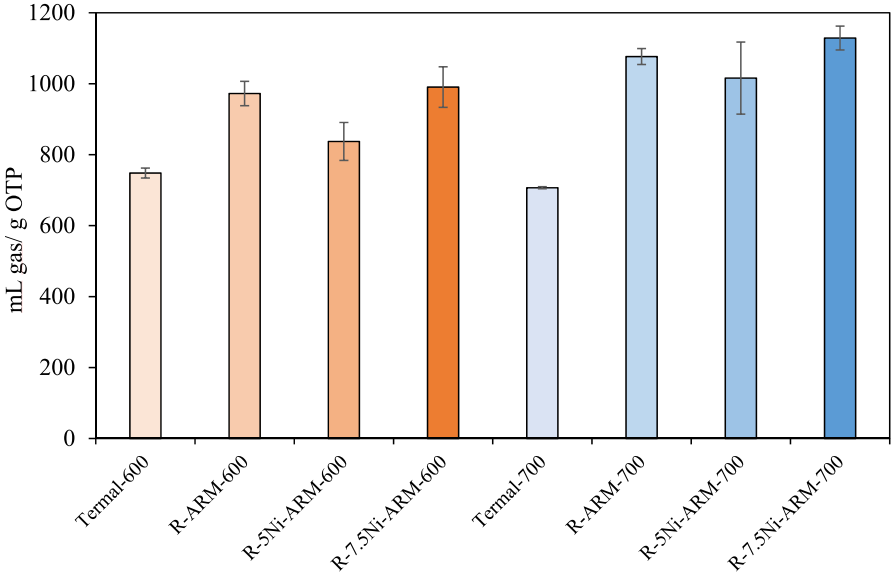

Fig. 5. Effect of Ni content of Ni-RM catalyst and catalytic bed temperature on H_2 yield.

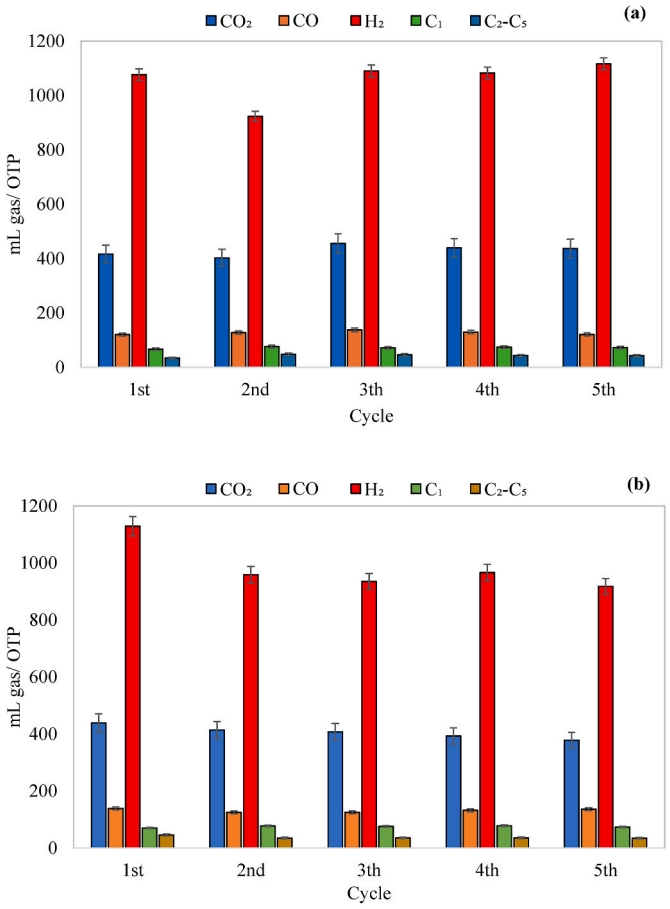

Fig. 6. Gas yields from cyclic test of (a) RR-ARM and (b) RR-7.5Ni-ARM.

approximately 15 % in the first cycle and remained almost the same in subsequent trials. The reason is probably due to the agglomeration phenomenon of nickel during regeneration, which leads to the reduction of catalytic activity [25].

4. Conclusion

In this work, a series of red mud-based catalysts were prepared, and applied in the ex-situ upgrading of volatiles (including tar) steam gasification of a lignocellulosic biomass. The gas product yield, especially H_2, were dependent on catalyst preparation techniques (thermal and plasma), nickel loading amount and process temperature. The iron oxide in RM and nickel oxide in Ni/RM underwent changes after the thermal reduction process by hydrogen, converting to magnetite, metallic iron and nickel. The thermal reduced RM alone showed almost the same activity with Ni-RM on the H_2 yield, suggesting that magnetite is effective catalyst for steam reforming.

Catalyst bed temperature also affected the H_2 yield. As the catalyst bed temperature increased from 600 °C to 700 °C, the H_2 yield increased by 11 % for the R-ARM catalyst and 14–21 % for the Ni-RM catalysts.

The required temperature for the complete reduction of Fe_2O_3 and Ni ions in the non-thermal plasma process could not be reached. Therefore, compared to thermal gasification, almost the same amount of H_2 yields were obtained with catalyst prepared in the presence of plasma. After four reaction/regeneration cycles, the regenerated R-RM catalyst provided the production of a hydrogen-rich gas with almost the same yield as the trial in which fresh catalyst was used. However, in the case of regenerated R-7.5Ni-ARM, the H_2 yield decreased by approximately 15 % compared to the yield obtained with fresh catalyst. More research is needed to understand why the activity of the R-Ni-ARM catalyst decreases in regeneration.

As a result, from the considerations that RM has negligible cost in price compared to nickel and noble metals and it is non-toxic, this study indicates that the thermal reduced RM could be effective catalyst for H_2 production from biomass for both economic and environmental reasons. To comprehensively determine the optimal conditions for steam gasification of OTP in the presence of R-ARM catalysts, a systematic experimental design should be employed in future studies, considering key variables such as temperature, steam to biomass ratio and biomass to catalyst ratio.

CRediT authorship contribution statement

Hakan Cay: Writing – original draft, Investigation, Formal analysis. **Nazire Merve Akbas:** Investigation. **Gozde Duman:** Writing – review & editing, Investigation, Formal analysis. **Osman Simsek:** Investigation. **Güray Yildiz:** Writing – review & editing, Investigation. **Weitao Wang:** Investigation. **Xin Tu:** Writing – review & editing, Funding acquisition. **Jale Yanik:** Writing – review & editing, Supervision, Investigation, Funding acquisition.

Declaration of competing interest

The authors declare that they have no known competing financial interests or personal relationships that could have appeared to influence the work reported in this paper.

Acknowledgements

This work was supported by an Institutional Links grant (British Council Newton Fund Institutional Links Grant, No. 623389161) under the Turkey partnership. The grant is funded by the UK Department for Business, Energy and Industrial Strategy together with the Scientific and Technological Research Council of Turkey (TÜBİTAK; Project No. 120N971) and delivered by the British Council. MATAL laboratories of Ege University and Integrated Research Centers of the Izmir Institute of Technology are acknowledged for catalyst characterization.

Appendix A. Supplementary data

Supplementary data to this article can be found online at https://doi.org/10.1016/j.renene.2025.123485.

References

[1] R.K. Goswami, S. Mehariya, P.K. Obulisamy, P. Verma, Advanced microalgae-based renewable biohydrogen production systems: a review, Bioresour. Technol. 320 (2021) 124301, https://doi.org/10.1016/j.biortech.2020.124301.
[2] P.K. Ghodke, A.K. Sharma, A. Jayaseelan, K.P. Gopinath, Hydrogen-rich syngas production from the lignocellulosic biomass by catalytic gasification: a state of art review on advance technologies, economic challenges, and future prospectus, Fuel 342 (2023) 127800, https://doi.org/10.1016/j.fuel.2023.127800.
[3] B. Li, C.F.M. Mbeugang, Y. Huang, D. Liu, Q. Wang, S. Zhang, A review of CaO based catalysts for tar removal during biomass gasification, Energy 244 (2022) 123172, https://doi.org/10.1016/j.energy.2022.123172.
[4] F.M. Alptekin, M.S. Celiktas, Review on catalytic biomass gasification for hydrogen production as a sustainable energy form and social, technological, economic, environmental, and political analysis of catalysts, ACS Omega 7 (2022) 24918–24941, https://doi.org/10.1021/acsomega.2c01538.
[5] Y. Lu, H. Jin, R. Zhang, Evaluation of stability and catalytic activity of Ni catalysts for hydrogen production by biomass gasification in supercritical water, Carbon Resour. Convers. 2 (1) (2019) 95–101, https://doi.org/10.1016/j.crcon.2019.03.001.
[6] J. Wang, D. Kang, B. Shen, H. Sun, C. Wu, Enhanced hydrogen production from catalytic biomass gasification with in-situ CO_2 capture, Environ. Pollut. 267 (2020) 115487, https://doi.org/10.1016/j.envpol.2020.115487.
[7] L.C.M. Ruivo, D.T. Pio, A.A. Yaremchenko, L.A.C. Tarelho, J.R. Frade, E. Kantarelis, K. Engvall, Iron-based catalyst (Fe2-xNixTiO5) for tar decomposition in biomass gasification, Fuel 300 (2021) 120859, https://doi.org/10.1016/j.fuel.2021.120859.
[8] L. Cheng, Z. Wub, Z. Zhang, C. Guo, N. Ellis, X. Bi, A.P. Watkinson, J.R. Grace, Tar elimination from biomass gasification syngas with bauxite residue derived catalysts

and gasification char, Appl. Energy 258 (2020) 114088, https://doi.org/10.1016/j.apenergy.2019.114088.
[9] T. Nordgreen, T. Liliedahl, K. Sjöström, Metallic iron as a tar breakdown catalyst related to atmospheric, fluidised bed gasification of biomass, Fuel 85 (2006) 689–694, https://doi.org/10.1016/j.fuel.2005.08.026.
[10] F. Zhang, Z. Song, J. Zhu, J. Sun, X. Zhao, Y. Mao, L. Liu, W. Wang, Factors influencing CH_4 single bond CO_2 reforming reaction over Fe catalyst supported on foam ceramics under microwave irradiation, Int. J. Hydrogen Energy 43 (2018) 9495–9502, https://doi.org/10.1016/j.ijhydene.2018.03.171.
[11] J. Wang, S. Zhang, D. Xu, H. Zhang, Catalytic activity evaluation and deactivation progress of red mud/carbonaceous catalyst for efficient biomass gasification tar cracking, Fuel 323 (2022) 124278, https://doi.org/10.1016/j.fuel.2022.124278.
[12] M. Mahinroosta, Z. Karimi, A. Allahverdi, Recycling of red mud for value-added applications: a comprehensive review, in: S. Hashmi, I.A. Choudhury (Eds.), Encyclopedia of Renewable and Sustainable Materials, Elsevier, 2020, pp. 561–582, https://doi.org/10.1016/B978-0-12-803581-8.11474-2.
[13] X. Zhou, L. Zhang, Q. Chen, X. Xiao, T. Wang, S. Cheng, J. Li, Study on the mechanism and reaction characteristics of red-mud-catalyzed pyrolysis of corn stover, Fuel 338 (2023) 127290, https://doi.org/10.1016/j.fuel.2022.127290.
[14] S. Wang, Z. Li, X. Bai, W. Yi, P. Fu, Catalytic pyrolysis of lignin with red mud derived hierarchical porous catalyst for alkyl-phenols and hydrocarbons production, J. Anal. Appl. Pyrolysis 136 (2018) 8–17, https://doi.org/10.1016/j.jaap.2018.10.024.
[15] S. Madadkhani, L. Burhenne, X. Bi, N. Ellis, J.R. Grace, T. Lewis, Bauxite residue as an iron-based catalyst for catalytic cracking of naphthalene, a model compound for gasification tar, Can. J. Chem. Eng. 99 (2021) 1461–1474, https://doi.org/10.1002/cjce.23872.
[16] E. Karimi, C. Briens, F. Berruti, S. Moloodi, T. Tzanetakis, M.J. Thomson, M. Schlaf, Red mud as a catalyst for the upgrading of hemp-seed pyrolysis bio-oil, Energy Fuels 24 (2010) 6586–6600, https://doi.org/10.1021/ef101154d.
[17] H. Jahromi, F.A. Agblevor, Hydrodeoxygenation of pinyon-juniper catalytic pyrolysis oil using red mud-supported nickel catalysts, Appl. Catal. B Environ. 236 (2018) 1–12, https://doi.org/10.1016/j.apcatb.2018.05.008.
[18] N. Yesilova, O. Tezer, A. Ongen, A. Ayol, Enhancing biomass gasification: a comparative study of catalyst applications in updraft and modifiable-downdraft fixed bed reactors, Int. J. Hydrogen Energy 76 (2024) 290–303, https://doi.org/10.1016/j.ijhydene.2024.05.075.
[19] X. Zhou, S. Cheng, Y. Li, C. Yang, L. Zhang, X. Xiao, T. Wang, Characterization and mechanism of red-mud-catalyzed steam gasification of corn stover, Fuel 356 (2024) 129611, https://doi.org/10.1016/j.fuel.2023.129611.
[20] A. Zhao, J. Lv, Q. Chen, Y. Xie, Y. Cao, C. Jiang, X. Ao, Spirit-based distillers' grains and red mud synergistically catalyse the steam gasification of anthracite to produce hydrogen rich synthesis gas, Int. J. Hydrogen Energy 46 (1) (2021) 314–323, https://doi.org/10.1016/j.ijhydene.2020.10.027.
[21] S. Dulger Irdem, E. Parparita, C. Vasile, M.A. Uddin, J. Yanik, Steam reforming of tar derived from walnut shell and almond shell gasification on red mud and iron-ceria catalysts, Energy Fuels 28 (2014) 3808–3813, https://doi.org/10.1021/ef500238f.
[22] H. Cay, G. Duman, J. Yanik, Two-step gasification of biochar for hydrogen rich gas production: effect of biochar type and catalyst, Energy Fuels 33 (8) (2019) 7398–7405, https://doi.org/10.1021/acs.energyfuels.9b01354.
[23] W. Dong, S. Li, M. Wang, X. Yuan, Y. Cao, X. Ao, Nickel-loaded red mud catalyst for steam gasification of bamboo sawdust to produce hydrogen-rich syngas, Int. J. Hydrogen Energy 48 (57) (2023) 21624–21635, https://doi.org/10.1016/j.ijhydene.2023.03.064.
[24] W. Tang, J.P. Cao, Z.M. He, W. Jiang, Z.H. Wang, X.Y. Zhao, Recent progress of catalysts for reforming of biomass tar/tar models at low temperatures – a short review, ChemCatChem 15 (2023) e202300581, https://doi.org/10.1002/cctc.202300581.
[25] Y. Wang, Y. Li, G. Wang, J. Zhu, H. Yang, L. Jin, S. Hu, H. Hu, In-situ catalytic upgrading of coal pyrolysis volatiles over red mud-supported nickel catalysts, Fuel 324 (2022) 124742, https://doi.org/10.1016/j.fuel.2022.124742.
[26] Y. Shen, P. Zhao, Q. Shao, F. Takahashi, K. Yoshikawa, In situ catalytic conversion of tar using rice husk char/ash supported nickel-iron catalysts for biomass pyrolytic gasification combined with the mixing-simulation in fluidized-bed gasifier, Appl. Energy 160 (2015) 808–819, https://doi.org/10.1016/j.apenergy.2014.10.074.
[27] X. Tu, H.J. Gallon, J.C. Whitehead, Plasma-assisted reduction of a NiO/Al_2O_3 catalyst in atmospheric pressure H_2/Ar dielectric barrier discharge, Catal. Today 211 (2013) 120–125, https://doi.org/10.1016/j.cattod.2013.03.024.
[28] J. Lian, X. Fang, W. Liu, Q. Huang, Q. Sun, H. Wang, X. Wang, W. Zhou, Ni supported on $LaFeO_3$ perovskites for methane steam reforming: on the promotional effects of plasma treatment in H_2–Ar atmosphere, Top. Catal. 60 (2017) 831–842, https://doi.org/10.1007/s11244-017-0748-6.
[29] J. Tyczkowski, H. Kierzkowska-Pawlak, Towards catalysts prepared by cold plasma, Catalysts 12 (2022) 75, https://doi.org/10.3390/catal12010075.
[30] Z. Wang, Y. Zhang, E.C. Neyts, X. Cao, X. Zhang, B.W.L. Jang, C.J. Liu, Catalyst preparation with plasmas: how does it work? ACS Catal. 8 (2018) 2093–2110, https://doi.org/10.1021/acscatal.7b03723.
[31] T.B. Gonoring, A.R. Franco, E.A. Vieira, R.C. Nascimento, Kinetic analysis of the reduction of hematite fines by cold hydrogen plasma, J. Mater. Res. Technol. 20 (2022) 2173–2187, https://doi.org/10.1016/j.jmrt.2022.07.174.
[32] M.A. Kougioumtzis, E. Karampinis, P. Grammelis, E. Kakaras, Integrated harvesting and biomass haulage of olive tree prunings. Evaluation of a two year harvesting campaign in Central Greece and fuel characterization of the prunings collected, Biomass Bioenergy 165 (2022) 106572, https://doi.org/10.1016/j.biombioe.2022.106572.
[33] J.M. Romero-García, J.C. López-Linares, M.M. Contreras, I. Romero, E. Castro, Exploitation of olive tree pruning biomass through hydrothermal pretreatments, Ind. Crop. Prod. 176 (2022) 114425, https://doi.org/10.1016/j.indcrop.2021.114425.
[34] B.G. Fonseca, S. Mateo, I.C. Roberto, S. Sánchez, A.J. Moya, Bioconversion in batch bioreactor of olive-tree pruning biomass optimizing treatments for ethanol production, Biochem. Eng. J. 164 (2020) 107793, https://doi.org/10.1016/j.bej.2020.107793.
[35] ASTM, Standard Test Methods for Determination of Carbon, Hydrogen and Nitrogen in Analysis Samples of Coal and Carbon in Analysis Samples of Coal and Coke, ASTM D5373-16, 2016.
[36] NREL, Determination of ash in biomass: laboratory analytical procedure (LAP). https://www.nrel.gov/docs/gen/fy08/42622.pdf, 2008.
[37] ASTM, Standard Test Method for Volatile Matter in the Analysis Sample of Coal and Coke, ASTM D3175-89a, 1997.
[38] S.A. Channiwala, P.P. Parikh, A unified correlation for estimating HHV of solid, liquid and gaseous fuels, Fuel 81 (2002) 1051–1063, https://doi.org/10.1016/S0016-2361(01)00131-4.
[39] DIN 51733, Testing of solid mineral fuels - ultimate analysis and calculation of oxygen content, DIN (2016).
[40] S. Liu, Plasma gas cleaning processes for the conversion of model tar from biomass gasification. Phd Thesis, Department of Electrical Engineering and Electronics, the University of Liverpool, 2017, p. 171p.
[41] R.C.C. Costa, F.C.C. Moura, P.E.F. Oliveira, F. Magalhães, J.D. Ardisson, R.M. Lago, Controlled reduction of red mud waste to produce active systems for environmental applications: Heterogeneous fenton reaction and reduction of Cr (VI), Chemosphere 78 (2010) 1116–1120, https://doi.org/10.1016/j.chemosphere.2009.12.032.
[42] C. Martos, J. Dufour, A. Ruiz, Synthesis of Fe_3O_4-based catalysts for the high temperature water gas shift reaction, Int. J. Hydrogen Energy 34 (2009) 4475–4481, https://doi.org/10.1016/j.ijhydene.2008.08.042.
[43] X. Liu, X. Yang, C. Liu, P. Chen, X. Yue, S. Zhang, Low-temperature catalytic steam reforming of toluene over activated carbon supported nickel catalysts, J. Taiwan Inst. Chem. Eng. 65 (2016) 233–241, https://doi.org/10.1016/j.jtice.2016.05.006.
[44] N. Gao, J. Salisu, C. Quan, P. Williams, Modified nickel-based catalysts for improved steam reforming of biomass tar: a critical review, Renew. Sustain. Energy Rev. 145 (2021) 111023, https://doi.org/10.1016/j.rser.2021.111023.